Reaction Kinetics, Mechanisms and Catalysis (2022) 135:1349–1364
https://doi.org/10.1007/s11144-022-02202-0

Iodine clocks: applications and untapped opportunities in materials science

Guido Panzarasa[1]

Received: 17 January 2022 / Accepted: 14 March 2022 / Published online: 24 March 2022

Abstract

Iodine clocks are fascinating nonlinear chemical systems with a glorious past and a promising future. The dynamic removal of iodine from these systems by different means can have important consequences for their reaction dynamics, and could be exploited for time-controlled autonomous dissipative self-assembly. Here, the untapped opportunities offered by iodine clocks for materials science, especially for the time-programming of supramolecular assembly and sol–gel transition, are reviewed and discussed with the hope of arousing the interest on the subject and stimulating new research directions.

Keywords Clock reactions · Systems chemistry · Soft matter · Autocatalysis · Supramolecular complexation · Gels

Introduction

Iodine clocks are chemical systems in which iodine[1] is a reaction product (the "clock species") which becomes measurable after a certain time lag. The changes in iodine concentration can be associated with changes in pH and redox potential. Following the taxonomy proposed by Horváth and Nagypál [1], it is then possible to distinguish between substrate-depletive clocks (e.g. the iodide–hydrogen peroxide–thiosulfate system, Landolt-type systems), autocatalysis-driven clocks (e.g. the iodate–thiocyanate reaction) and pseudo-clocks (e.g. the chlorite–iodide reaction). Here we take the liberty to introduce the expression "inverse iodine clock" to indicate systems, such as the chlorite–iodide reaction, in which iodine consumption rather than production is the main kinetic event.

[1] The terms iodine and triiodide will be used interchangeably throghout the text, unless they'll need to be distinguished for the sake of clarity.

✉ Guido Panzarasa
guidop@ethz.ch

[1] Wood Materials Science, Institute for Building Materials, ETH Zürich, Laura-Hezner-Weg 7, 8093 Zurich, Switzerland

Despite their unquestionably great relevance for the field of chemical kinetics itself [2], for the development of analytical tests [3], and for pedagogical demonstrations [4], clock reactions and oscillating chemical systems in general (not only "iodine" ones) have not yet received the attention they deserve from the materials science community. The goal of the present work is to discuss, without claiming to be exhaustive, the relevance of iodine sequestration for iodine clocks and how this can lead to great opportunities for materials-oriented applications.

Relevance of iodine complexation in iodine clock systems

The solubility of iodine I_2 in water is relatively low (around 0.29 g L^{-1} at 20 °C [5]), but it reacts readily with iodide ions I^- to form the triiodide ion I_3^- (and other poly(iodides)), a relatively hydrophobic charge–transfer complex, according to the equilibrium (Eq. 1):

$$I_2 + I^- \rightleftharpoons I_3^- \tag{1}$$

The addition of I_3^--complexing agents to a mixture of iodine and iodide can increase the formation of triiodide by disrupting this equilibrium. The ability of iodine to form supramolecular complexes with a variety of small (e.g., cyclodextrins) and polymeric molecules (e.g., amylose, poly(ethylene glycol) PEG, poly(vinyl pyrrolidone) PVP, poly(vinyl alcohol) PVA) is very well known [6]. Its relevance, both theoretical and practical, is great in fields as diverse as medicine (e.g. topical antiseptics, radiopaque materials), materials science (e.g. polarizers, electrochemical cells) and, obviously, analytical chemistry (the iodine–starch test, iodometry).

Among iodine–polymer complexes, the one with amylose (a component of starch) is possibly one of the most popular thanks to its usefulness as a color test. The intense blue-black color of the iodine–amylose complex has been used to mark the set-off times of iodine clocks since the pioneering work of Harcourt and Esson in 1866 [7]. However, the subtle effects of iodine removal (including by means of complex formation) on the dynamics of iodine clocks started to be recognized only from the 1990s.

Discussing the oscillations produced by the iodate–hydroxylamine reaction in a continuous-flow stirred tank reactor (CSTR), in 1990, Rábai and Epstein explicitly mentioned the effect of dynamic iodine removal from the system, in that case by volatilization, on the reaction behavior and made a relevant hypothesis:

> The essential role of iodine evaporation is another special feature of this system. The removal of one species from the CSTR, not only by the common output flow but also selectively in another way, may be a useful approach to generating new oscillators. Evaporation of bromine plays a key role in several modified BZ-type oscillator in a closed system. One may also envision systems in which the selective removal occurs not to the gas phase but to an immiscible liquid phase or by precipitation, as may occur with MnO_2, in the family of permanganate oscillators. Perhaps the most important instances of

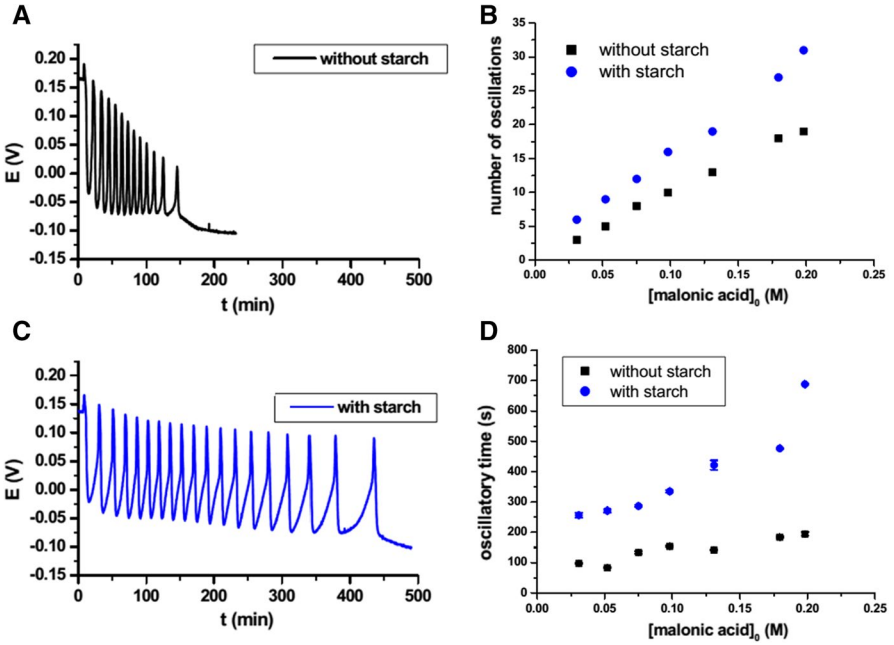

Fig. 1 **A**, **B** Oscillations recorded in a Briggs–Rauscher mixture without (**A**) and with (**B**) 0.48 mg mL^{-1} of starch. **C**, **D** Effect of malonic acid concentration on the oscillations number (**C**) and time (**D**) in presence and absence of 0.48 mg mL^{-1} of starch. Reproduced and adapted with permission from [14]

this phenomenon may occur in biological oscillators where different products can be excreted through membranes at very different rates. [8]

It is noteworthy that iodine removal by volatilization plays a central role also in the decomposition of acidic hydrogen peroxide catalysed by iodate and iodine, that is the Bray–Liebhafsky (BL) system [9, 10], the first known homogeneous oscillating chemical reaction. The BL reaction features oscillations in iodine concentration, and bursts of oxygen. These latter, apart from complicating the reaction mechanism, contribute to iodine losses due to evaporation, which in turn influence the oscillating behavior of the system [11, 12].

In the oscillating Briggs–Rauscher (BR) system (which involves hydrogen peroxide, iodate, divalent manganese Mn^{2+} as a catalyst and malonic acid as a substrate), starch is often used to show the abrupt increase in iodide as a sudden change from amber (free iodine) to dark blue (amylose–triiodide complex) [13]. Recently, however, the passive role of starch has been questioned by the work of Csepei and Bolla [14]. Compared to the starch-free BR system, both the number and the period of oscillations increased in presence of starch, and the iodine consumption (by reaction with malonic acid) within one period of oscillation was also significantly slower. Thus, it is suggested that in the BR system starch might act as an iodine reservoir, affecting the reaction steps in which iodine is involved (Fig. 1).

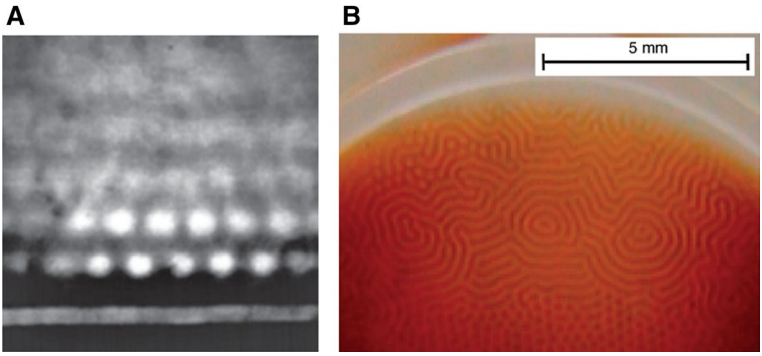

Fig. 2 Turing patterns enabled by iodine sequestration in the CIMA reaction performed in open gel reactors. The iodine-complexing agent is **A** starch (historical image from December 1989, reprinted with permission from [20]), **B** a co-polymer containing *N*,*N*-dimethylaminoethylacrylate methyl chloride quaternary salt. Reprinted with permission from [19]. Copyright 2011 American Chemical Society

Back in 1990, "the first unambiguous experimental evidence of a Turing structure" was reported by Boissonade, De Kepper and collaborators for the chlorite–iodine–malonic acid (CIMA) reaction in an open gel reactor [15] (Fig. 2A). Two years later, Lengyel and Epstein were able to rationalize the formation of such reaction–diffusion patterns as resulting from the

> introduction of a reagent that reversibly forms an unreactive, immobile complex with the activator species […] making it possible to produce Turing patterns in systems that would not otherwise exhibit such structures [16].

That reagent was starch, which by complexing iodine acted at the same time as a visual indicator and reduced the effective diffusion coefficient of the activator (iodide) relative to the inhibitor (chlorite), allowing the formation of Turing patterns. Further studies showed that the same effect could be obtained by substituting starch with PVA [17], or using highly-crosslinked gels [18]. More recently, quaternary alkylammonium cationic amphiphiles, both as micelles (*n*-dodecyltrimethylammonium bromide) and as polymers (based on *N*,*N*-dimethylaminoethylacrylate methyl chloride quaternary salt) incorporated in inert gels were also used to generate Turing patterns, trapping the iodide activator as counterion and reducing its diffusivity [19] (Fig. 2B).

The CIMA reaction is not the only system allowing to produce spatiotemporal patterns by iodine trapping. In 1994, Horváth and Showalter used α-cyclodextrin (α-CD), another iodine-complexing agent, to alter the diffusivity of the autocatalyst iodide in the iodate-arsenous acid (IAA) reaction in a gel medium, leading to lateral instabilities and the formation of cellular fronts on otherwise stable waves. The use of gelled media suppressed hydro-dynamic effects, generating pure reaction–diffusion fronts [21]. In 2002, Forštová et al. investigated in more detail the effect of complexation with starch on front propagation in the gelled IAA system and how it modifies the structures produced when an electric field is applied. They showed, by means of both experiments and simulations, that

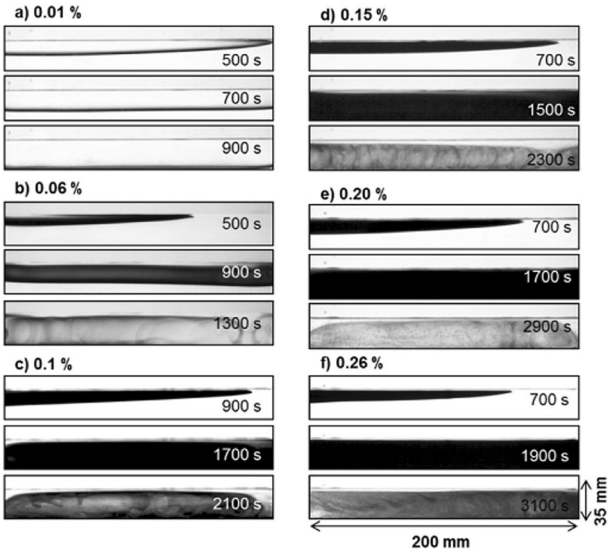

Fig. 3 Evolution of experimentally observed patterns in the IAA reaction for different starch concentrations. Reproduced with permission from [23]

> […] starch, usually considered as an inert compound utilized only to indicate the progress of the wave propagation and the mixture composition, actually affects the propagation velocity and, when an electric field is applied, the reaction stoichiometry as well. We assumed that starch enters the reaction–diffusion mechanism via the formation of immobile complexes with both I_2 and I_3^-. The addition of starch reduces the effective diffusion coefficients of some of the reacting species, […] slowing down the velocity of propagation of the fronts, with a greater reduction in speed as more starch is used in the reaction mixture. [22]

In 2017, Sebestikova et al. [23] reported a similar tendency for a non-gelled IAA reaction system, in which the fronts propagated due to the reaction–diffusion–convection coupling. A decrease of both vertical and horizontal velocities was observed for increasing starch concentration up to 0.15%, then the velocity became independent from starch concentration, suggesting that only a certain amount of the produced iodine is available for the complexation reaction (Fig. 3). Under such conditions, the iodine-generating Dushman reaction [24] (Eq. 2) should produce locally an amount of iodine higher than that could be immediately consumed by the Roebuck reaction [25] (Eq. 3):

$$IO_3^- + 5I^- + 6H^+ \rightarrow 3I_2 + 3H_2O \tag{2}$$

$$H_3AsO_3 + I_2 + H_2O \rightarrow H_3AsO_4 + 2I^- + 2H^+ \tag{3}$$

A dramatic effect of iodine sequestration by complex formation was recently demonstrated also for the chlorite–iodide (CI) reaction, an "inverse iodine clock" in which the accumulation of iodine is accompanied by its abrupt disappearance. Its basic mechanism has been established in 1906 by Bray [26] (Eqs. 4–6):

$$ClO_2^- + 4I^- + 4H^+ \rightarrow 2I_2 + Cl^- + 2H_2O \quad (4)$$

$$5ClO_2^- + 2I_2 + 2H_2O \rightarrow 4IO_3^- + 5Cl^- + 4H^+ \quad (5)$$

$$5ClO_2^- + I_2 \rightarrow 2IO_3^- + 3Cl^- + 2ClO_2 \quad (6)$$

Further kinetic investigations made by Kern and Kim in 1965 pointed out the role of iodine as an autocatalyst [27]. The CI reaction is best known for its "crazy clock" [28] (or "pseudo-clock" [1]) behavior, that is irreproducible time lag, due to a high sensitivity to mixing conditions.

In 2019, Panzarasa et al. [29] reported an innovative study on the effect of iodine sequestration on the CI reaction (Fig. 4). Instead of carrying out the chlorite–iodide reaction in acetate buffer ($pH \leq 5$), δ-gluconolactone (GL, a cyclic ester) was used as a slow acid generator (Eq. 7).

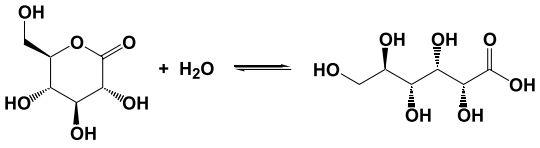

(7)

In these conditions, the pH increased alongside iodine formation but then dropped upon the sudden disappearance of the latter. The dynamics of this transient pH change were found to be dependent on the cyclic ester concentration (Fig. 4A and B). Moreover, iodine complexation was achieved by substituting the iodide salt (usually sodium or potassium) with tetraalkylammonium (or phosphonium) iodides with different linear aliphatic chain lengths (from methyl to butyl). Quaternary ammonium (or phosphonium) cations interact electrostatically with the negatively charged, hydrophobic triiodide ions, forming salts with a water solubility depending on the aliphatic chain length, in the order: methyl ≈ ethyl ≫ propyl ≫ butyl. Thus, using tetrapropyl- and tetrabutylammonium (or phosphonium) iodides as reactants, iodine precipitates and the reaction course can be followed by turbidity measurements. The sequestration of iodine resulted in delayed, less intense and more broadened pH bursts (Fig. 4C and D), possibly because of the role of iodine as an autocatalyst. Similar behavior was observed using sodium iodide as a reactant and α-CD as complexing agent.

Iodine sequestration by precipitation can be achieved also through the formation of insoluble metal iodides, such as mercury(II) iodide or silver(I) iodide. This approach has been used to investigate intermediate reaction species (e.g. in the BL reaction [30]) as well as to delay or inhibit the appearance of iodine in the Landolt reaction, as in the popular "Old Nassau" demonstration [31]. A dramatic inhibitory

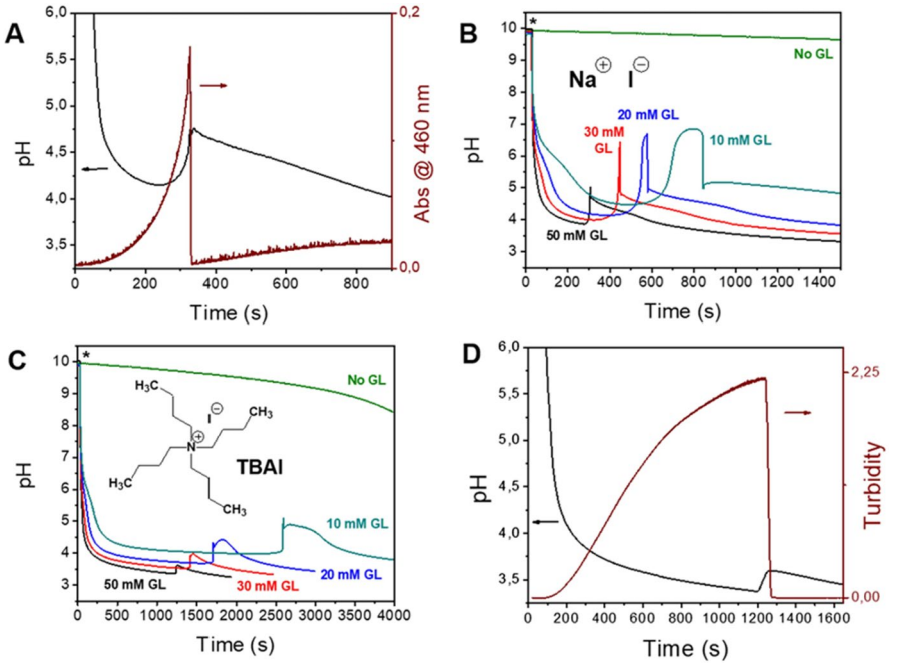

Fig. 4 **A** Evolution of iodine concentration (from the absorbance at 460 nm) and pH over time for the chlorite–iodide (CI) reaction in the presence of 50 mM δ-gluconolactone (GL). **b** Evolution of pH over time for the CI reaction with decreasing GL concentrations. **C** Evolution of turbidity and pH over time for the chlorite-tetrabutylammonium iodide (C-TBAI) reaction in the presence of 50 mM GL. **D** Evolution of pH for the C-TBAI reaction with decreasing GL concentrations. The moment of GL addition is marked by an asterisk. Reproduced from [29], with the permission of AIP Publishing

effect of mercury and silver ions on the iodate–arsenious acid reaction has also been reported [32].

Applications of iodine clocks to materials systems

Nonlinear and periodic (bio)chemical phenomena are widespread in living systems. They are necessary to regulate and maintain vital processes such as cyrcadian rhytms, hormonal cycles, and homeostasis, as well as to grow structures. Living organisms are masters of making complex materials through a careful and selective use of feedback processes such as autocatalysis and self-inhibition, leading to spatiotemporal organization continuously fueled by dissipation of chemical energy. The design of artificial dissipative self-assembly systems is a way to mimic these processes and, as such, is one of the most attractive and challenging fields of research in contemporary materials science [33]. Of the different clock reactions that have been

applied to colloidal and soft materials to make programmable autonomous dissipative systems [34–42], here the focus will be given to iodine-based ones.

Colloidal systems

Possibly the first report on the deliberate use of an iodine clock to trigger self-assembly by supramolecular iodine complex formation is a demonstration published in 1967, in which poly(ethylene glycol) (PEG, 4 kDa) is used to precipitate the iodine generated by the Landolt (iodate–bisulfite) reaction (Eq. 8) [43]:

$$IO_3^- + 3HSO_3^- \rightarrow I^- + 3SO_4^{2-} + 3H^+ \quad (8)$$

From the original article [44]:

> Add *B* [mix 5.0 mL of 0.08 M KIO_3 (in 0.5 M H_2SO_4) with 50 mL of water] to *A* [mix 4.0 mL of 0.25 M $NaHSO_3$ with 100 mL of 5% aq-polyethylene glycol (PEG 4000)] and swirl briefly to mix the solutions. Immediately on mixing a homogeneous water-white solution results, which after a short time instantaneously turns to a yellowish-red color. A second or so later there is an instataneous formation of a chocolate-brown precipitate. The effects are dramatic and demonstrate the liberation of precipitating agent (yellowish-red triiodide ion) followed by the pptn. of the PEG–Iodine complex. At room temperature the color changes in 15–17 s. The time may be changed by altering the temperature or the concentrations. […] Polyethylene glycol polymers (PEG) $HOCH_2$ . . $(CH_2OCH_2)_N$ . . CH_2OH are water soluble and quantitatively precipitate iodine when $N \geq 67$. ($N = 67$ to 83 for PEG 4000). It is proposed that one mole of iodine is bound to each ether linkage and these 1 : 1 insoluble complexes are similar to those in diethyl ether.

The idea of coupling an iodine clock with iodine complexation was re-explored in 2016 by Wang et al. for the dissipative self-assembly of supra-amphiphiles [45]. A hydrophilic block copolymer, methoxy-poly(ethylene glycol)$_{113}$-block-poly(L-lysine hydrochloride)$_{200}$ (PEG-b-PLKC), was used to generate a supra-amphiphile PEG(I_2)-b-PLKC. Upon iodine complexation, the amphiphilicity of the PEG segment changed from hydrophilic to hydrophobic while the PLKC segment remained hydrophilic, resulting in the formation of colloidal aggregates. These spherical aggregates could be detected only for an iodine concentration ≥ 0.06 mM, corresponding to *ca.* 6.6% of the total PEG repeating units, and their diameter (measured by dynamic light scattering, DLS) was found to decrease for increasing iodine concentrations. A positive (+22.5 mV) zeta potential of the aggregates indicated the orientation towards the surface of the PLKC block, which could contribute to electrostatic stabilization. The formation of a PEG-I_2 complex was confirmed by ^{1}H-NMR as a dramatic weakening and broadening of the otherwise sharp CH_2 peak of the PEG block at $\delta = 3.6$ ppm. Thanks to this iodine-responsive behavior, a dissipative self-assembly could be obtained by coupling PEG-b-PLKC with a iodate–hydroxylamine oscillator in CSTR conditions, able to generate iodine in a time-dependent way without degrading the copolymer (Fig. 5A and B). Upon the

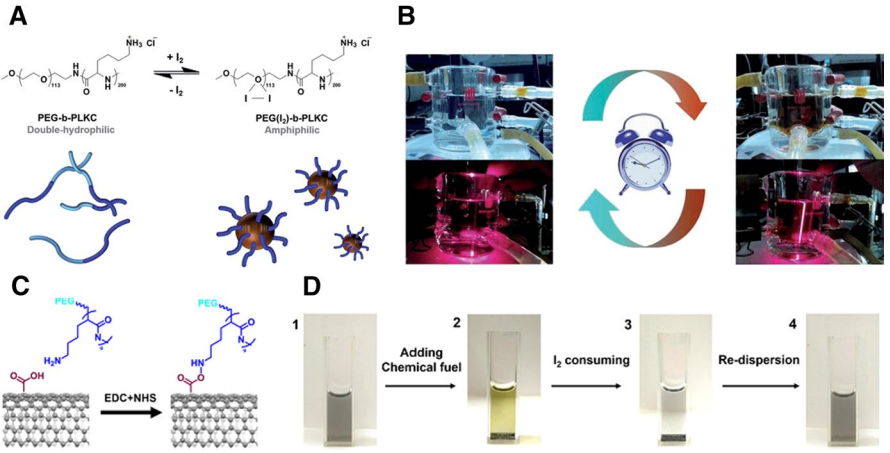

Fig. 5 **A** Schematic representation and **B** photographic sequence for the PEG(I_2)-b-PLKC supra-amphiphile formation. Reprinted (adapted) with permission from [45]. **C** Schematic representation of the preparation of supra-amphiphilic MWCNTs. **D** Photographic sequence showing the transient aggregation and redispersion of supra-amphiphilic MWCNTs. The aggregation happens very fast upon addition of the "chemical fuel", while the redispersion can take from around 30 min to more than 1 h, depending on the concentration of reactants. Reprinted (adapted) with permission from [46]. Copyright 2018 American Chemical Society

addition of PEG-b-PLKC to the iodate–hydroxylamine system, the period of the oscillations changed from 5.3 h to about 3.2 h. Although not discussed explicitly by the authors, this behavior can be easily rationalized as an effect of iodine sequestration: while in the original work of Rábai and Epstein [8] this was due to iodine volatilization, in this case it was achieved by complex formation.

In a follow-up paper, also by Wang et al. [46], the transient self-assembly of PEG(I_2)-b-PLKC supra-amphiphile was studied in batch conditions instead of using a CSTR. To trigger the assembly, an unbuffered mixture of iodate and thiourea (the "fuel") was added to a solution of PEG-b-PLKC, iodide and acid. Upon mixing, I_2 was rapidly produced by the Dushman reaction between iodate and iodide, resulting in a slight increase of pH. The coordination of I_2 with the PEG segment of the block copolymer then resulted in the formation and self-assembly of the polymeric supra-amphiphile PEG(I_2)-b-PLKC, as already discussed. Meanwhile, thiourea would slowly reduce I_2 to iodide by two acid-generating reactions (Eqs. 9, 10):

$$I_2 + 2\left(NH_2\right)_2CS \rightarrow H_2N(NH)CSSC(NH)NH_2 + 2I^- + 2H^+ \tag{9}$$

$$7I_2 + H_2N(NH)CSSC(NH)NH_2 + 14H_2O \rightarrow 2SO_4^{2-} + 2CO_3^{2-} + 14I^- + 4NH_4^+ + 18H^+ \tag{10}$$

The rate of iodine consumption was mainly determined by reaction (10) and could be easily followed in time by UV–Vis spectrophotometry. Meanwhile, the formation and dissolution of the aggregates could be observed by DLS. Changing the concentration of thiourea allowed to tune the lifetime of the transient aggregates,

but had no impact on their average size. Furthermore, the aggregates could be reformed multiple times by repeated additions of the iodate–thiourea solution to the reaction system after I_2 was fully consumed, but the system showed fatigue (that is, shorter lifetimes) due to accumulation of unreacted thiourea and increased iodide concentration.

In the same work, the influence of PEG and PLKC blocks length on the self-assembly of PEG(I_2)-b-PLKC was also studied. By decreasing the chain length of PEG from 113 to 23, the diameter of the transient assemblies formed by $PEG_{23}(I_2)$-b-$PLKC_{200}$ was much larger (> 200 nm) compared to that of $PEG_{113}(I_2)$-b-$PLKC_{200}$ ones (~90 nm). Notably, $PEG_{23}(I_2)$-b-$PLKC_{200}$ could only assemble into a few loose and irregularly-shaped aggregates (as shown by transmission electron microscopy), and DLS measurements suggested that their lifetime was shorter than that of the assemblies formed by $PEG_{113}(I_2)$-b-$PLKC_{200}$. These differences may be due to the lower hydrophobicity and reduced stability of the iodine complex with PEG of lower molecular weight, in accordance with previous studies [44, 47]. On the other hand, the length of the $PLKC_n$ segment (n = 100 or 200) did not have an effect as straightforward on the size, shape and lifetime of the transient aggregates.

Eventually, a proof-of-concept application of the iodine clock-controlled dissipative self-assembly of PEG_{113}-b-$PLKC_{200}$ was demonstrated by grafting the block copolymer onto carboxylated multiwalled carbon nanotubes (MCNTs). The resulting modified MCNTs were found to transiently aggregate upon the addition of the "chemical fuel" (iodate-thiourea solution), removing a model organic pollutant (rhodamine B) from water. Upon I_2 consumption, the modified MCNTs would spontaneously redisperse and could be used for another cycle of pollutant removal (Fig. 5C and D).

Gel systems

Gels have countless technological uses, from food to medicine, from energy generation to environmental remediation, from additive manufacturing to artificial tissues and organs. Gels are integral components of cellular living organisms, which have evolved a stunning ability to control the mechanical properties (viscosity, stiffness) of their cytoplasm, thanks to spatio-temporal control of gel formation as well as dissolution, as a result of internal metabolism (e.g. bacteria) or for movement purposes (e.g. amoebas). The design of systems with time-programmed sol–gel transitions is thus of exceptional theoretical and applicative relevance. However, tuning the time of sol–gel transition without compromising the structure and properties of the final gel remains challenging.

Clock and oscillating reactions have been coupled to pre-made gels to obtain chemomechanical oscillations, such as in the seminal 1996 paper of Yoshida and collaborators on the BZ-powered self-oscillating gel [48], or as described in the excellent 2014 work of Horváth where synergetic chemomechanical oscillations were obtained by coupling pH-responsive gels with the Landolt iodine clock in a CSTR reactor [49]. The usefulness of pH clocks and kinetic switches to control gelation in time has been demonstrated using slow acid generators, such as

δ-gluconolactone [50], or, most often, using enzymatic systems such as urease-urea [51, 52].

Panzarasa, Riedel and collaborators were the first to report, in 2021, a new approach based on controlling supramolecular gelation with iodine clocks [41, 42]. Poly(vinyl alcohol) is known to make supramolecular complexes with iodine, very similar to those formed by amylose [53]. The addition of 5% PVA (130 kDa) to a

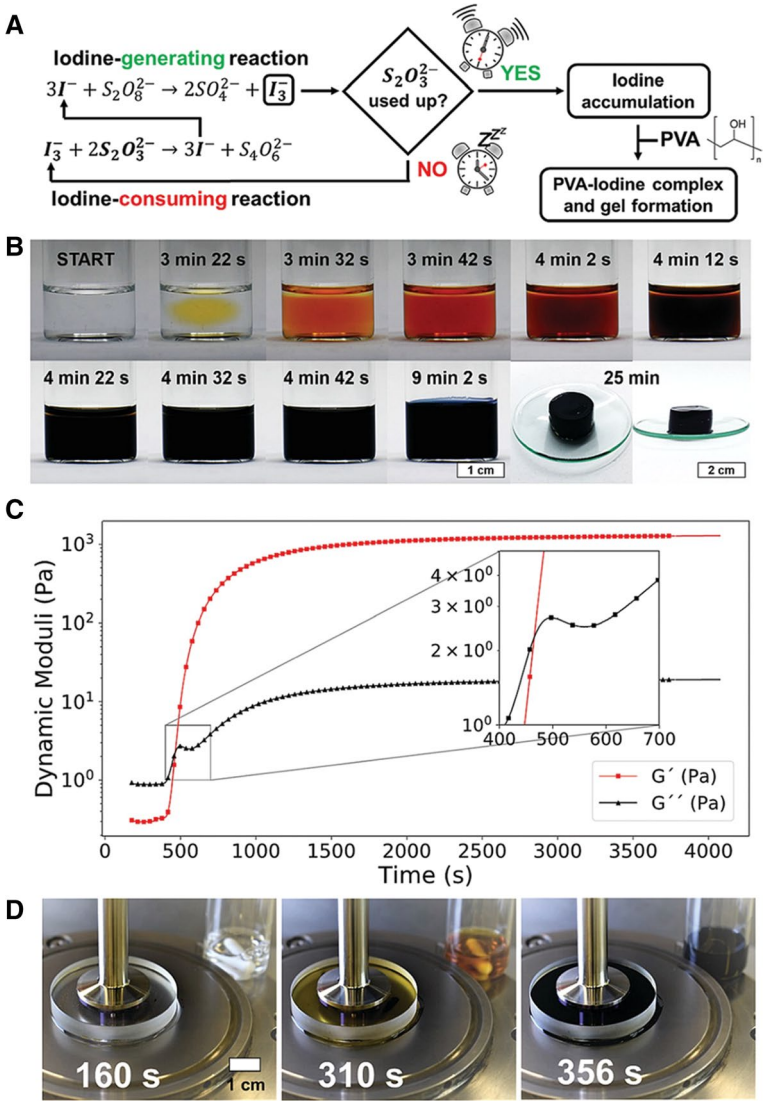

Fig. 6 **A** Mechanism of the IPT–PVA system. **B** Photographic sequence showing a typical color evolution and gel formation in the IPT-PVA system. **C** Dynamic time sweep curve showing the evolution of elastic and dissipative shear moduli during gel formation. In (**D**) the corresponding photographic sequence (transparent rheometer plate) is shown. Reproduced and adapted with permission from [41]

Fig. 7 **A** Simplified reaction mechanism of the iodate–HMS–PVA system. **B–D** Self-propagating reaction fronts in the iodate–HMS–PVA system, showing the effect of the concentration of iodate and HMS on the formation of a stable gel, a transient gel, or of no gel (only free iodine). The green and red frames symbolize the predominant reaction pathway. The reaction is started by pipetting 7 µL of 50 mM sodium bisulfate, and the moment the acid drop touches the mixture is set as time $t = 0$. **E** Photographic sequence showing the formation of a stable PVA–I_2 gel with δ-gluconolactone GL as slow acid generator. **F**, **G** Rheology plots of the iodate–HMS–PVA system with different concentrations of **F** GL, **G** sodium bisulfate as acid triggers. **H** Front instabilities and spatio-temporal patterns observed in the iodate–HMS–PVA system. The light green and pink colors of the reaction mixture are due to pH indicators (methyl yellow and bromocresol green). Reproduced and adapted with permission from [42] ▶

classical iodide–persulfate–thiosulfate (IPT) system led to the formation of stable PVA-I_2 gels after an induction time governed by the iodine clock (Fig. 6A and B).

The IPT system is a substrate-depletive iodine clock, in which the appearance of iodine from the reaction between iodide and persulfate is retarded until complete consumption of the thiosulfate. The accumulating iodine then complexes with PVA. The crucial finding was that, in presence of a sufficiently high amount of PVA of suitable molecular weigth, this would eventually result in the formation of a stable network i.e. a gel. Thanks to the initial lagtime, it was possible to study the whole sol–gel transition process by means of rheology (Fig. 6C and D). The gelation time as well as the final mechanical properties of the gel could be tailored by tuning the iodine clock parameters, the molecular weight of PVA and by introducing competitive iodine complexing agents, such as methyl-β-cyclodextrin. Furthermore, the gel was stable in water (due to the low solubility of iodine), but could be easily dissolved in presence of substances able to decompose iodine (e.g. thiosulfate) or extracting it in solution (e.g. methyl-β-cyclodextrin) [41].

Substituting the IPT clock with the iodate–hydroxymethanesulfinate (iodate–HMS) reaction led to another breakthrough, that is the discovery of frontal supramolecular polymerization [42]. The iodine clock behavior of the iodate–HMS system has been previously studied by Simoyi and collaborators, who identified also its acid- and iodine-autocatalyzed behavior (Fig. 7A) [54]. As other autocatalysis-driven systems (e.g. the IAA and CI reactions), the iodate–hydroxymethanesulfinate reaction can be very sensitive to the reaction stoichiometry. In a relatively narrow range of concentrations, this reaction could behave either as an iodine clock or as an inverse iodine clock. Based on the results obtained with the IPT clock, Panzarasa and Riedel decided to investigate the effect of PVA addition on the reaction. To their delight, it resulted in the generation of self-propagating gels, stable or autonomously transient depending on the reaction conditions (Fig. 7B–D). It was found that the reaction could be either triggered by the external addition of acid, or programmed to activate autonomously using slow acid generators such as δ-gluconolactone. Furthermore, in the iodate–hydroxymethanesulfinate–PVA system, thanks to autocatalysis, both gel formation (Fig. 7E–G) and dissolution happen much faster compared to the IPT–PVA system, and spatio-temporal patterns can also emerge (Fig. 7H).

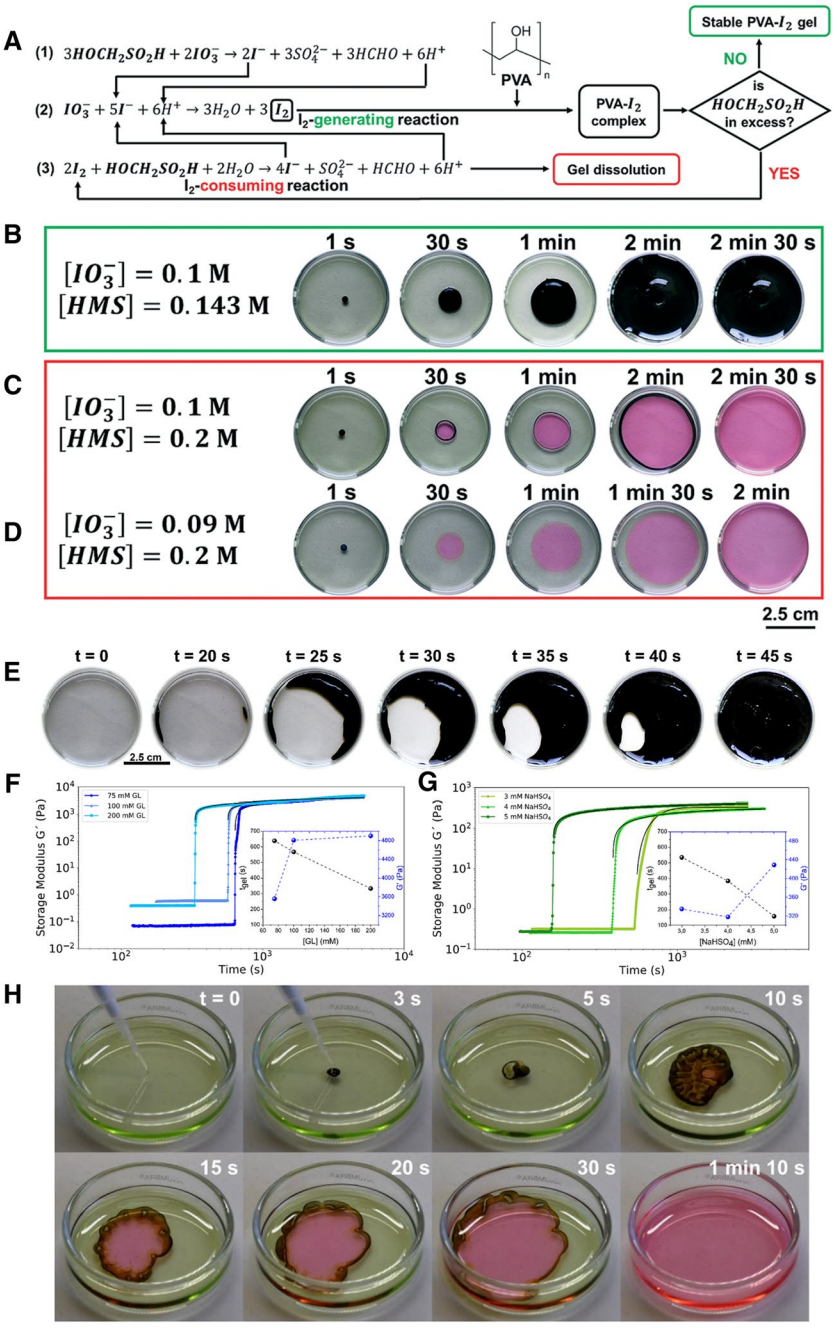
A
(1) $3HOCH_2SO_2H + 2IO_3^- \rightarrow 2I^- + 3SO_4^{2-} + 3HCHO + 6H^+$
(2) $IO_3^- + 5I^- + 6H^+ \rightarrow 3H_2O + 3I_2$
I2-generating reaction
(3) $2I_2 + HOCH_2SO_2H + 2H_2O \rightarrow 4I^- + SO_4^{2-} + HCHO + 6H^+$
I2-consuming reaction
PVA
PVA-I2 complex
Gel dissolution
Stable PVA-I2 gel
NO
is $HOCH_2SO_2H$ in excess?
YES
B
$[IO_3^-] = 0.1$ M
$[HMS] = 0.143$ M
1 s
30 s
1 min
2 min
2 min 30 s
C
$[IO_3^-] = 0.1$ M
$[HMS] = 0.2$ M
D
$[IO_3^-] = 0.09$ M
$[HMS] = 0.2$ M
1 min 30 s
2.5 cm
E
t = 0
t = 20 s
t = 25 s
t = 30 s
t = 35 s
t = 40 s
t = 45 s
F
Storage Modulus G´ (Pa)
Time (s)
75 mM GL
100 mM GL
200 mM GL
[GL] (mM)
G
3 mM NaHSO4
4 mM NaHSO4
5 mM NaHSO4
[NaHSO4] (mM)
H
t = 0
3 s
5 s
10 s
15 s
20 s
30 s
1 min 10 s

Conclusions

A variety of complex kinetic phenomena can arise from the coupling of iodine clocks with supramolecular complexation, which can be exploited for the time-programming of supramolecular assembly and sol–gel transitions. This opens up new horizons for the design and development of active and adaptive materials. Given the huge variety of iodine clocks already known, the overincreasing interest for far-from-equilibrium materials systems and the ability to program their autonomous behavior in time, already the examples discussed here demonstrate how productive this approach could be. Although it is difficult at present to divine what could be the next groundbreaking discoveries in this regard, it might be reasonable to point out at the use of time-controlled supramolecular iodine complexation for developing novel metal–iodine batteries [55] and thermo-electrochemical cells [56].

Acknowledgements Solenn Riedel, Ronny Kürsteiner, Prof. Dr. Ingo Burgert and Prof. Dr. Eric Dufresne are kindly acknowledged for their support. This work is dedicated to Ugoberto and Huguette. Part of the research described here was funded by the ETH Career Seed Grant SEED-12 20-1.

Funding Open access funding provided by Swiss Federal Institute of Technology Zurich.

References

1. Horvath AK, Nagypal I (2015) Classification of clock reactions. ChemPhysChem 16:588–594
2. King MC (1981) Experiments with time: progress and problems in the development of chemical kinetics. Ambix 28:70–82
3. Prabhu GRD, Witek HA, Urban PL (2018) Chemical clocks, oscillations, and other temporal effects in analytical chemistry: oddity or viable approach? Analyst 143:3514–3525
4. Carpenter Y, Phillips HA, Jakubinek MB (2010) Clock reaction: outreach attraction. J Chem Educ 87:945–947
5. Hartley H, Campbell NP (1908) LXIX—the solubility of iodine in water. J Chem Soc Trans 93:741–745. https://doi.org/10.1039/CT9089300741
6. Moulay S (2013) Molecular iodine/polymer complexes. J Polym Eng 33:389–443. https://doi.org/10.1515/polyeng-2012-0122
7. Harcourt VA, Esson W (1867) VII. On the laws of connexion between the conditions of a chemical change and its amount. Philos Trans 157:117–137
8. Rabai G, Epstein IR (1990) Large amplitude pH oscillation in the oxidation of hydroxylamine by iodate in a continuous-flow stirred tank reactor. J Phys Chem 94:6361–6365
9. Bray WC (1921) A periodic reaction in homogeneous solution and its relation to catalysis. J Am Chem Soc 43:1262–1267. https://doi.org/10.1021/ja01439a007
10. Bray WC, Liebhafsky HA (1931) Reactions involving hydrogen peroxide, iodine and iodate ion. I. Introduction. J Am Chem Soc 53:38–44

11. Sevcik P, Kissimonova K, Adamcikova L (2000) Oxygen production in the oscillatory Bray–Liebhafsky reaction. J Phys Chem A 104:3958–3963
12. Schmitz G (1999) Effects of oxygen on the Bray–Liebhafsky reaction. Phys Chem Chem Phys 1:4605–4608
13. Briggs TS, Rauscher WC (1973) An oscillating iodine clock. J Chem Educ 50:496. https://doi.org/10.1021/ed050p496
14. Csepei LI, Bolla C (2015) Is starch only a visual indicator for iodine in the Briggs–Rauscher oscillating reaction? Stud UBB Chem 60:187–199
15. Castets V, Dulos E, Boissonade J, De Kepper P (1990) Experimental evidence of a sustained standing Turing-type nonequilibrium chemical pattern. Phys Rev Lett 64:2953–2956
16. Lengyel I, Epstein IR (1992) A chemical approach to designing Turing patterns in reaction–diffusion systems. Proc Natl Acad Sci USA 89:3977–3979
17. Noszticzius Z, Quyang Q, McCormick WD, Swinney LH (1992) Effect of Turing pattern indicators on CIMA oscillators. J Phys Chem 96:6302–6307
18. Kyoung JL, McCormick WD, Swinney HL, Noszticzius Z (1992) Turing patterns visualized by index of refraction variations. J Chem Phys 96:4048
19. Asakura K, Konishi R, Nakatani T et al (2011) Turing pattern formation by the CIMA reaction in a chemical system consisting of quaternary alkyl ammonium cationic groups. J Phys Chem B 115:3959–3963
20. Szalai I, Cuinas D, Takacs N et al (2012) Chemical morphogenesis: recent experimental advances in reaction–diffusion system design and control. Interface Focus 2:417–432
21. Horvath D, Showalter K (1995) Instabilities in propagating reaction-diffusion fronts of the iodate-arsenous acid reaction. J Chem Phys 102:2471–2478
22. Forštová L, Ševčíková H, Merkin JH (2002) The influence of the starch indicator on front waves in the iodate–arsenous acid system with applied electric fields. Phys Chem Chem Phys 4:2236–2245
23. Sebestikova L, Simcik M, Ruzicka MC (2017) Effects of the starch indicator on the buoyantly unstable iodate-arsenous acid reaction front. ChemistrySelect 2:7141–7149
24. Dushman S (1904) The rate of the reaction between iodic and hydriodic acids. J Phys Chem 8:453–482
25. Roebuck JR (1905) The rate of the reaction between arsenious acid and iodine in acid solution, the rate of the reverse reaction, and the equilibrium between them. J Phys Chem 9:727–763
26. Bray WC (1906) Beiträge zur Kenntnis der Halogensauerstoffverbindungen. Abhandlung IV. Die Reaktion zwischen Chlordioxyd und Jodion. Zeitschrift für Phys Chemie 54U:731–749
27. Kern DM, Kim C-H (1965) Iodine catalysis in the chlorite-iodide reaction. J Am Chem Soc 87:5309–5313
28. Nagypal I, Epstein IR (1988) Stochastic behavior and stirring rate effects in the chlorite–iodide reaction. J Chem Phys 89:6925
29. Panzarasa G, Dufresne ER (2019) Impact of in situ acid generation and iodine sequestration on the chlorite–iodide clock reaction. Chaos 29:071102
30. Furrow S (1987) Reactions of iodine intermediates in iodate-hydrogen peroxide oscillators. J Phys Chem 91:2129–2135
31. Alyea HN (1977) The old Nassau reaction. J Chem Educ 54:167–168
32. Bognar J, Sarosi S (1963) Bestimmung von jodid auf grund seiner katalytischen wirkung mittels der jodat-arsenit-reaktion. Anal Chim Acta 29:406–414
33. Epstein IR, Xu B (2016) Reaction-diffusion processes at the nano- and microscales. Nat Nanotechnol 11:312–319
34. Panzarasa G, Dufresne ER (2020) Temporal control of soft materials with chemical clocks. Chimia (Aarau) 74:612
35. Panzarasa G, Osypova A, Sicher A et al (2018) Controlled formation of chitosan particles by a clock reaction. Soft Matter 14:6415–6418. https://doi.org/10.1039/c8sm01060a
36. Panzarasa G, Torzynski AL, Sai T et al (2020) Transient supramolecular assembly of a functional perylene diimide controlled by a programmable pH cycle. Soft Matter 16:591–594. https://doi.org/10.1039/c9sm02026h
37. Panzarasa G, Sai T, Torzynski AL et al (2020) Supramolecular assembly by time-programmed acid autocatalysis. Mol Syst Des Eng 5:445–448
38. Panzarasa G (2020) Clocking the clock: programmable acid autocatalysis in the chlorite-tetrathionate reaction. ChemistrySelect 5:8074–8077

39. Osypova A, Duebner M, Panzarasa G (2020) Oscillating reactions meet polymers at interfaces. Materials (Basel) 13:2957
40. Sproncken CCM, Gumi-Audenis B, Panzarasa G, Voets IK (2020) Two-stage polyelectrolyte assembly orchestrated by a clock reaction. ChemSystemsChem 2:e2000005. https://doi.org/10.1002/syst.202000005
41. Riedel S, Schweizer T, Smith-Mannschott K et al (2021) Supramolecular gelation controlled by an iodine clock. Soft Matter 17:1189–1193. https://doi.org/10.1039/d0sm02285c
42. Riedel S, Panzarasa G (2021) Stable and transient self-propagating supramolecular gelation. Mol Syst Des Eng 6:883–887. https://doi.org/10.1039/d1me00116g
43. Landolt H (1887) Ueber die Zeitdauer der Reaction zwischen Jodsaure und schwefliger Saure. Berichte der Dtsch Chem Gesellschaft 20:745–760. https://doi.org/10.1002/cber.188702001173
44. Hiskey CF, Cantwell FF (1967) Instantaneous precipitation from homogeneous solution. J Chem Educ 44:A727
45. Wang G, Tang B, Liu Y et al (2016) The fabrication of a supra-amphiphile for dissipative self-assembly. Chem Sci 7:1151–1155. https://doi.org/10.1039/c5sc03907j
46. Wang G, Sun J, An L, Liu S (2018) Fuel-driven dissipative self-assembly of a supra-amphiphile in batch reactor. Biomacromol 19:2542–2548
47. Hiskey CF, Cantwell FF (1966) Interaction of aqueous polyethylene glycol solutions with iodine. J Pharm Sci 55:166–168
48. Yoshida R, Takahashi T, Yamaguchi T, Ichijo H (1996) Self-oscillating gel. J Am Chem Soc 118:5134–5135. https://doi.org/10.1021/ja9602511
49. Horváth J (2014) Sustained large-amplitude chemomechanical oscillations induced by the landolt clock reaction. J Phys Chem B 118:8891–8900. https://doi.org/10.1021/jp5050964
50. Adams DJ, Butler MF, Frith WJ et al (2009) A new method for maintaining homogeneity during liquid-hydrogel transitions using low molecular weight hydrogelators. Soft Matter 5:1856–1862. https://doi.org/10.1039/b901556f
51. Jee E, Bánsági T, Taylor AF, Pojman JA (2016) Temporal control of gelation and polymerization fronts driven by an autocatalytic enzyme reaction. Angew Chemie - Int Ed 55:2127–2131. https://doi.org/10.1002/anie.201510604
52. Mai AQ, Bánsági T, Taylor AF, Pojman JA (2021) Reaction-diffusion hydrogels from urease enzyme particles for patterned coatings. Commun Chem 4:101
53. Zwick MM (1966) The blue complexes of iodine with poly(vinyl alcohol) and amylose. J Polym Sci Part A 4:1642–1644. https://doi.org/10.1002/pol.1966.150040626
54. Ojo JF, Otoikhian A, Olojo R, Simoyi RH (2004) Oxyhalogen-sulfur chemistry: nonlinear oxidation kinetics of hydroxymethanesulfinic acid by acidic iodate. J Phys Chem A 108:2457–2463. https://doi.org/10.1021/jp037140q
55. Yang J, Song Y, Liu Q, Tang A (2021) High-capacity zinc–iodine flow batteries enabled by a polymer–polyiodide complex cathode. J Mater Chem A 9:16093–16098
56. Zhou H, Yamada T, Kimizuka N (2018) Thermo-electrochemical cells empowered by selective inclusion of redox-active ions by polysaccharides. Sustain Energy Fuels 2:472–478. https://doi.org/10.1039/c7se00470b